Received: *April 7, 1998*, Accepted: *May 7, 1998*

Comparison of improved and unimproved quenched hadron spectroscopy

Attilio Cucchieri, Tereza Mendes and Roberto Petronzio*

Dipartimento di Fisica, Università di Roma "Tor Vergata"
and INFN, Sezione di Roma II
Via della Ricerca Scientifica 1, 00133 Rome, Italy

Abstract: We make a comparison between our quenched-hadron-spectroscopy results for the non-perturbatively-improved Wilson action and the corresponding unimproved case, at $\beta = 6.2$ on the same set of gauge configurations. Within our statistics, we find in the improved case a baryon spectrum closer to experimental data and a better stability in the determination of the strange-quark mass.

Keywords: Nonperturbative Effects, Lattice QCD.

*Alternative address: CERN, Theory Division, CH-1211 Geneva 23, Switzerland.

JHEP05(1998)006

A full agreement of lattice QCD simulations with the experimental results is only expected when the continuum limit is taken and the full unquenched theory, including the effects of fermion loops, is simulated. The quenched approximation has been shown to reproduce the basic pattern of the QCD spectrum, although quantitative studies still reveal deviations from the experimental results that can be ascribed to the lack of fermion loops or to the lattice artifacts affecting the quenched approximation away from the continuum limit.

The computation cost of the extrapolation to the continuum limit of lattice QCD simulations can be significantly reduced by using improved actions, where the leading cutoff effects are cancelled by suitable counterterms. It has been shown that on-shell improvement of O(a) is achieved by adding to the usual Wilson action the clover term, with a coefficient that has been determined non-perturbatively by the ALPHA collaboration [1].

The scope of this paper is to compare the results of the non-perturbatively-improved Wilson action with respect to the usual, unimproved, action. The former is less affected by lattice artifacts and an agreement of an improved quantity with the experimental data is taken as a sign of the usefulness of the improvement programme. In general, improved results do not need to agree better with experimental data: when they reduce the discrepancy they also reduce the expected effect of fermion loops.

A real check of the faster approach to the continuum of the improved results can only be obtained by studying the dependence upon the lattice spacing, i.e. by working at different values of the bare coupling. This systematic study is beyond the scope of our paper. We work at a single value of β and we take advantage of a comparison made on the same set of gauge configurations. This allows a jackknife analysis of the difference between improved and unimproved data directly.

A detailed analysis of our results for the improved case has appeared elsewhere [2], and here we concentrate on the comparison between the two cases (a preliminary study can be found in [3]). We refer to [1] for the description of the improvement programme.

We consider a lattice of volume $24^3 \times 48$ and coupling $\beta = 6.2$. We choose the following values for the hopping parameter κ in the unimproved case: 0.1350, 0.1400, 0.1450, 0.1506, 0.1510, 0.1517, 0.1526 (for the improved case we used: 0.1240, 0.1275, 0.1310, 0.1340, 0.1345, 0.1350, 0.1352). The highest κ values correspond to the strange-quark mass region: results for lighter quark masses are only obtained by extrapolation. We consider, for the improved as well as for the unimproved case, all nondegenerate flavor combinations from the different values of κ. Our simulations were carried out on the 512-processor computer of the APE100 series at the University of Rome "Tor Vergata".

Our statistics come from 104 quenched gauge configurations, generated by a hybrid over-relaxation algorithm, with each update corresponding to a heat-bath sweep followed by three over-relaxation sweeps. The configurations are separated by 1000 updates. The numerical inversion of the propagator for the improved case is described in [2]. For the unimproved case we have performed the inversion in a similar manner, but for the last part of our configurations we have implemented the SSOR algorithm [4], which corresponds roughly to a gain of a factor 4 in the inversion time.

The analysis of the data for the improved case is described in [2]. For the unimproved case, we have followed the same procedure, namely hadron masses are obtained from single-mass fits to the large time behaviour of zero-momentum hadron correlators, and the errors are estimated through a single-elimination jack-knife procedure.

We remark that we determine κ_c for both cases by using the so-called Ward identity mass m_{WI}, considered in [2] (in the unimproved case we set the coefficient c_A to zero). We thus obtain for the unimproved case the value

$$\kappa_c = 0.153230(9) \quad (\text{from } m_{WI} = 0). \tag{1}$$

This may be compared with the value $\kappa_c = 0.153291(15)$, obtained from $M_{PS}^2 = 0$.

For the fits to the dependence of hadron masses upon quark masses we use in the unimproved case the bare quark mass, defined as $m_q(\kappa) \equiv (1/\kappa - 1/\kappa_c)/2$, while for the improved case we use an improved bare quark mass [1] defined by

$$\widetilde{m}_q(\kappa) \equiv m_q(\kappa)\,[1 + b_m\, m_q(\kappa)]\ . \tag{2}$$

(Note that $\widetilde{m}_q$ is the renormalized mass with $Z_m = 1$.) The improvement coefficient b_m has been determined non-perturbatively [5] to be $b_m = -0.62(3)$. For non-degenerate-flavour cases, we use symmetric averages of the masses defined above.

We use physical inputs at the strange-quark mass for the lattice spacing. This avoids the inclusion of systematic uncertainties deriving from a chiral extrapolation. The value of the strange-quark mass in lattice units is obtained by using a fit to the ratio M_{PS}^2/M_V^2 at the experimental value $(M_K/M_{K^*})^2$. We get for the unimproved case the value

$$m_s = 0.0316(47)\ , \tag{3}$$

to be compared with the improved case [2]: $m_s = 0.0315(45)$.

The inverse lattice spacing a^{-1} in MeV is then obtained by normalizing the K^* mass to its experimental value. We get

$$a_{K^*}^{-1} = \frac{M_{K^*}}{M_V(m_s/2)} = 2943(100)\ \text{MeV}, \tag{4}$$

to be compared with the result obtained in the improved case with the same definition [2]: $a_{K^*}^{-1} = 2561(100)$. (The values for a^{-1} coming from M_ρ (the chiral value) and M_ϕ are obtained similarly, by linear extrapolation/interpolation.)

We show in Table 1 the values of the various ratios of different determinations of a^{-1} and their jack-knife errors. The difference is between the unimproved value and the improved case. The jack-knife errors of the differences were computed as follows: we consider these differences for each cluster of configurations (obtained by single elimination), and we then evaluate their jack-knife errors. A distinctive difference between the

JHEP05(1998)006

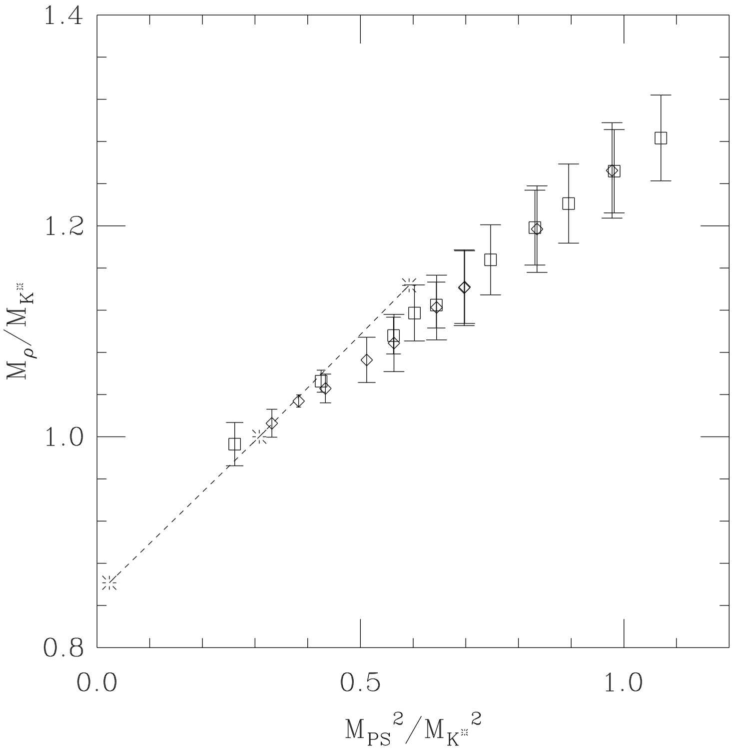

Figure 1: APE plot for M_V. The improved case ($\diamond$) is compared with the unimproved one ($\square$).

	unimproved	improved	difference
$r_1 \equiv a_{K^*}^{-1}/a_\rho^{-1}$	1.037(23)	1.030(33)	0.007(27)
$r_2 \equiv a_\phi^{-1}/a_{K^*}^{-1}$	1.030(31)	1.029(27)	0.0008(270)
$r_3 \equiv a_\phi^{-1}/a_\rho^{-1}$	1.067(56)	1.060(62)	0.008(54)

Table 1: Ratios of different determinations of the inverse lattice spacing a^{-1}

two cases cannot be observed within our statistics, but for the ratio r_1, whose deviation from unity in the improved case is more significant than in the unimproved one.

In Fig. 1 we show a plot of the vector-meson mass as a function of M_{PS}^2 for the two cases. The masses are normalized to the K^*-meson mass, taken at the strange-quark mass value given in eq. (3) above. The asterisks correspond to the experimental values, i.e. the vector-meson masses M_ρ , M_{K^*} , M_ϕ , and appropriate combinations of pseudoscalar-meson masses. The errors in the plot are calculated from independent jack-knife procedures in the two cases. The difference between improved and unimproved simulations can be made statistically significant only if a jack-knife procedure is applied to the parameters of a fit. Indeed, the values of kappa where the inversions were taken did correspond to different quark masses and a direct jack-knife procedure for the hadron masses is not possible.

As can be seen from Fig. 1, the experimental slope dM_V/dM_{PS}^2 is different from the one corresponding to our data (this happens for the improved as well as for the

	exp.	unimproved	improved	difference
J_{K^*}	0.487	0.382(48)	0.391(66)	-0.0081(525)
J_ϕ	0.557	0.409(44)	0.427(54)	-0.019(44)

Table 2: Comparison of values of the quantity J

	unimproved	improved	difference
m_c/m_s	12.58(190)	10.11(140)	2.47(140)

Table 3: Our lattice data for the ratio of charm-quark over strange-quark masses

unimproved case). This slope is related to the behaviour of the dimensionless quantity J defined by [6]:

$$J \equiv M_V \,(dM_V/dM_{PS}^2) \;, \tag{5}$$

obtained from M_V as a function of M_{PS}^2. A comparison of the J values for the two cases is made in Table 2. Again, the difference was computed for each cluster, and only then was its jack-knife error evaluated. We see that the improvement on J is marginal, which seems to indicate that the discrepancy between the lattice data and the experimental values should come from the quenching approximation.

We also consider the charm-quark mass m_c, which we obtain from a fit to the ratio $M_{PS}^2/M_{K^*}^2$ (the experimental input $M_D^2/M_{K^*}^2$ is used). We show in Table 3 a comparison of the ratio m_c/m_s between the improved and the unimproved case. Note that this is also the ratio of renormalized quark masses, since in the ratio of charm- over strange-quark mass the renormalization factor Z_m drops out.

The value of the lattice strange-quark mass given in eq. (3) and the ratio m_c/m_s in Table 3 can be used to obtain two independent determinations of the physical mass of the strange quark, as explained in [2]. The two resulting values in the full theory are expected to agree, provided that they are evolved through the renormalization-group equation to the same scale. Both strange and charm lattice quark masses are determined from heavy-light states whose basic energy scale is fixed by the light quark rather than the heavy. The difference of the two determinations comes from the way the physical units for the strange-quark mass are obtained. In the first definition, the physical units to the strange-quark mass are given by the lattice spacing fixed by the strange-meson spectroscopy, and in the second case by the physical value of the charm quark mass determined in charmonium calculations. Therefore, in the first case, the quark mass is obtained at the scale of the lattice spacing, and in the second case at the scale of the charm quark mass. The evolution to the common scale where the comparison is made, conventionally chosen to be 2 GeV, is performed with the full beta function including the effects of fermion loops. This gives, in the unimproved case:

$$m_s^{(1)} = 115(13) \text{ MeV} \quad \text{from } m_s \tag{6}$$

$$m_s^{(2)} = 87(13) \text{ MeV} \quad \text{from } m_c/m_s \,, \tag{7}$$

JHEP05(1998)006

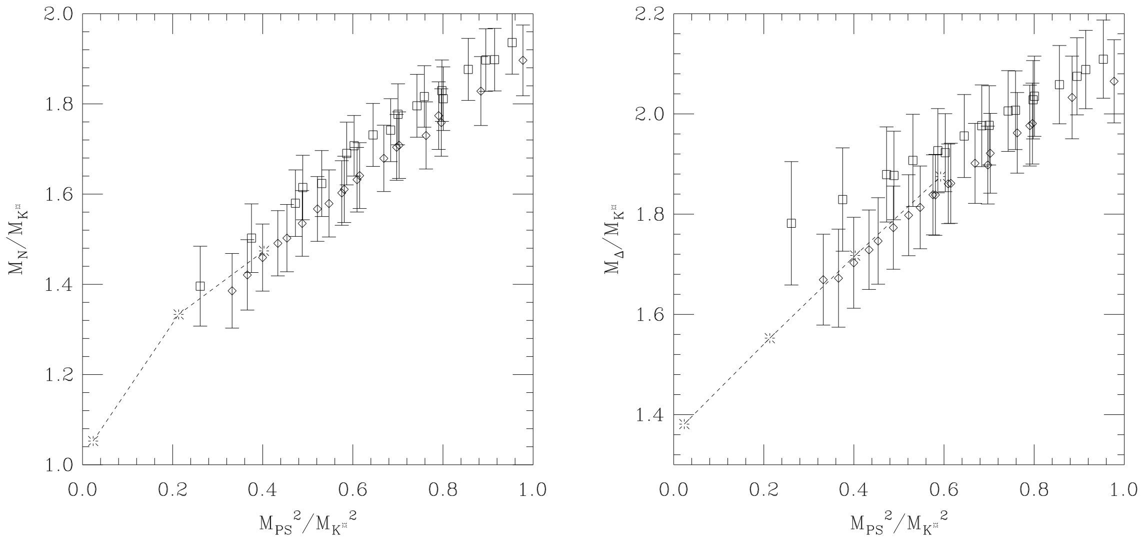

Figure 2: APE plot for (a) the nucleon mass (octet baryons) and (b) the Δ mass (decuplet baryons). The improved case ($\diamond$) is compared with the unimproved one ($\square$).

	unimproved	improved	difference
$m_s^{(1)}/m_s^{(2)}$	1.315(56)	1.005(49)	0.310(48)

Table 4: The ratio of the two strange-quark mass determinations

while for the improved case (using the improved bare quark mass $\widetilde{m}_q$) we obtained [2]: $m_s^{(1)} = 111(15)$ MeV and $m_s^{(2)} = 111(16)$ MeV.

In order to compare the improved and unimproved cases, we consider the dimensionless ratio $m_s^{(1)}/m_s^{(2)}$. Our results are shown in Table 4. We see a clear improvement here. This comes from two different sources: the variation of the lattice spacing (which influences the determination of $m_s^{(1)}$), and the use of the improved bare quark mass (which mainly affects the determination of $m_s^{(2)}$).

We now turn to the comparison of baryonic observables. We consider non-degenerate flavour combinations, and therefore we can draw APE plots with several values of the hadron mass. Plots are shown in Fig. 2 for the nucleon (or more precisely the Σ-like octet baryons) and for the Δ (decuplet baryons). We refer to [2] for details on how our baryon masses are obtained. Again, masses are normalized to the K^* meson mass. Experimental points in these figures (asterisks) correspond to M_N, M_Σ and M_Ξ and appropriate meson masses in Fig. 2a, and similarly M_Δ, M_{Σ^*},M_{Ξ^*} and M_Ω for Fig. 2b. The quark-mass dependence of the decuplet is positively affected by the improvement.

In Table 5 we give some of our baryon mass values in MeV (for convenience, we also include the improved values already reported in [2]). The difference between unimproved and improved results can be taken for each cluster as was done before; we consider dimensionless ratios formed by the baryon mass divided by M_{K^*}, in order to erase the uncertainty coming from the determination of the lattice spacing in the two

	exp.	unimproved	improved
M_N	939	1054(90)	952(110)
$M_{\Sigma-\Lambda}$	73.7	49(25)	70(30)
M_Δ	1232	1495(125)	1265(110)
$M_{\Delta-N}$	293	336(55)	297(80)

Table 5: Baryon masses in MeV (improved and unimproved) and comparison with experiment. The error in parentheses represents the statistical error, while the error due to the determination of the inverse lattice spacing is of about 4%

	exp	unimproved	improved	difference
M_N/M_{K^*}	1.05	1.18(11)	1.07(13)	0.11(13)
$M_{\Sigma-\Lambda}/M_{K^*}$	0.083	0.054(26)	0.079(33)	-0.024(33)
M_Δ/M_{K^*}	1.38	1.68(17)	1.42(13)	0.26(12)
$M_{\Delta-N}/M_{K^*}$	0.33	0.38(7)	0.33(9)	0.044(70)

Table 6: Jack-knife comparison between improved and unimproved dimensionless ratios of baryon masses divided by a reference physical mass scale.

cases. The results are shown in Table 6. The improved results are in better agreement with the experimental points.

In the determination of baryon mass splittings we have made fits directly to the ratio of correlations in order to minimize the effects of collective fluctuations. Our study of these mass splittings follows that of Ref. [7], in particular for the choice of a quadratic fit as a function of the bare quark mass for the Σ-Λ splitting normalized by the difference of the heaviest and the lightest quark mass.[1] We show plots of these fits for the unimproved and the improved case in Fig. 3. The Δ-N splitting and the individual baryon masses were well fitted by a linear function.

The use of a non-perturbatively-improved action leads to a systematic smaller but comparable spread in the value of the lattice spacing extracted from light mesons with and without strange quarks. Within our statistics, it does not improve dramatically the meson spectrum, while it affects the baryon quark-mass dependence, especially for the decuplet, and moves it into a better agreement with the experimental data. This gives evidence that the main discrepancies for the baryon spectrum at lattice spacings of the order of 0.1 fm are likely mainly due to lattice artifacts than to fermion-loop effects. We have also found a remarkable agreement in the improved theory with respect to the unimproved case between two independent determinations of the strange-quark mass, one normalized through the lattice spacing and the other from the value for the charm mass extracted in the continuum from charmonium-spectrum calculations.

[1] The quadratic fit shows χ^2/dof values that are comparable to those of a linear fit with fewer (light-mass) points in the unimproved case and about three times smaller in the improved case, strongly suggesting a quadratic behaviour. The same was observed in Ref. [7].

JHEP05(1998)006

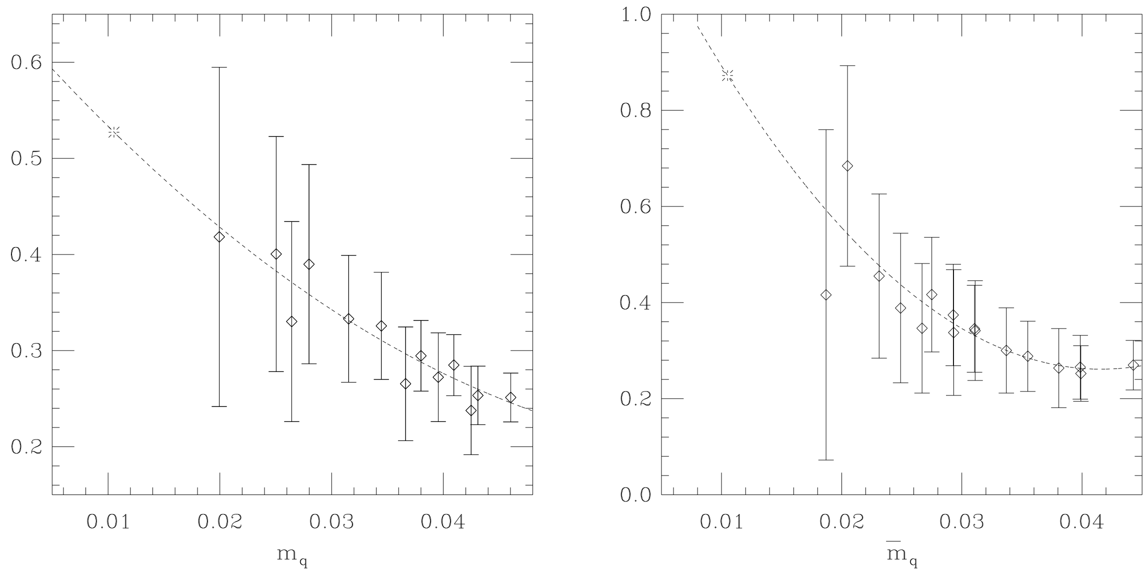

Figure 3: The Σ-Λ mass splitting (divided by the difference of the heaviest and the lightest quark masses) as a function of the average bare quark mass in lattice units, and the corresponding quadratic fit (dashed line) for: (a) the unimproved case and (b) the improved case. The asterisk corresponds to the extrapolated value at the physical point (two light and one strange quarks).

References

[1] M. Lüscher et al., *Nucl. Phys.* **B 478** (1996) 365 [`hep-lat/9605038`];
M. Lüscher et al., *Nucl. Phys.* **B 491** (1997) 323 [`hep-lat/9609035`].

[2] A. Cucchieri et al., *Phys. Lett.* **B 422** (1998) 212 [`hep-lat/9711040`].

[3] T. Mendes, *Nucl. Phys.* **63** *(Proc. Suppl.)* (1998) 170 [`hep-lat/9711023`].

[4] S. Fischer et al., *Comput. Phys. Commun.* **98** (1996) 20 [`hep-th/9602019`].

[5] G.M. de Divitiis and R. Petronzio, *Phys. Lett.* **B 419** (1998) 311 [`hep-lat/9710071`].

[6] L. Maiani and G. Martinelli, *Phys. Lett.* **B 178** (1986) 265;
P. Lacock et al., *Phys. Rev.* **D 52** (1995) 5213 [`hep-lat/9506009`].

[7] T. Bhattacharya et al., *Phys. Rev.* **D 53** (1996) 6486 [`hep-lat/9512021`].